IET Generation, Transmission & Distribution

Research Article

IET Journals
The Institution of Engineering and Technology

Development of leakage energy allocation approach for time-varying interharmonics tracking

ISSN 1751-8687
Received on 10th June 2014
Accepted on 17th November 2014
doi: 10.1049/iet-gtd.2014.0728
www.ietdl.org

Hsiung Cheng Lin ✉

Department of Electronic Engineering, National Chin-Yi University of Technology, Taichung, Taiwan
✉ *E-mail: hclin@ncut.edu.tw*

Abstract: Recently, an increasing use of power electronic facilities in industry has produced considerable harmonics and interharmonics in power systems. The power supply quality is therefore seriously threatened. The discrete Fourier transform (DFT) is currently the most important tool in signal analysis. However, a misapplication of DFT may result in incorrect outcome because of some inherent limitations such as spectral leakage or aliasing effect etc. The existing interharmonics even raise more difficulty in signal analysis than harmonics. To overcome this dilemma, this study develops a strategy of leakage energy allocation method for both stationary and non-stationary interharmonics identification. The proposed algorithm can regain its original interharmonics amplitude by restoring all spilled leakage energy, and also finds its individual frequency component according to the distribution of spilled leakage energy. The performance effectiveness of the proposed approach is verified using the numerical examples in terms of reliability, rapid response and high-precision performance.

1 Introduction

The fast growing use of power electronics equipment and periodical time-varying loads in electric power system has led to serious harmonics and interharmonics problems. Interharmonics can be thought of as the inter-modulation of the fundamental and harmonic components of the system, and their frequencies are not an integer of the fundamental components. They are generated by the loads that are not pulsating synchronously with the fundamental power system. Major sources have been found in variable-load electric drives, double conversion system, cycloconverters, time-varying loads, wind turbine and unexpected sources [1–5]. In addition to typical problems caused by harmonics, interharmonics create some new problems such as cathode ray tube (CRT) flicker, low-frequency oscillation in a mechanical system, voltage fluctuations etc. Even under low amplitude, the above phenomena may still exist [6–12].

The measurement of interharmonics does pose more difficulty than harmonics. This is mainly due to spectral leakage sensitivity, very low magnitude values in interests, waveform periodicity change, and time-variant frequencies and amplitudes. To address aforementioned measuring issues, IEC 61000-4-7 standard provides a guide line for interharmonics measurement by grouping methods, where 200 ms window width used for 12 cycles of 60 zHz systems and 10 cycles for 50 Hz systems [13]. A 5 Hz frequency resolution with rectangular window is suggested to be adopted. However, interharmonic frequencies may not be obtained accurately under this framework [14]. The point is that in this standard the central frequency of interharmonic group is defined as the group frequency. This results in no exact interharmonic frequency information available from the measurement.

Theoretically, it is not difficult to extensively apply some harmonic analysis methods to interharmonics measurement by the concept of Fourier transform [15–23]. In a practical circumstance, however, there are still many concerns as follows [24]: (i) It is not easy to extend to low power analogue model and time-domain model. (ii) Direct injection method may cause inaccurate outcome easily. (iii) Harmonic power flow method is very difficult in modelling a non-linear system if the signal contains interharmonics. (iv) Iterative harmonic analysis is unable to model non-linear load. For the above reasons, the research work in interharmonics measurement is still on the way [25–38].

2 Traditional measurement methods

2.1 Discrete Fourier transform (DFT) measurement

By Fourier theory, any repetitive waveform can be extended to a series of sine waveforms in different frequencies which are a multiple of fundamental system frequency. For a distorted waveform $i_s(t)$, it can be resprented using a complex number by

$$i_s(t) = \sum_{n=-\infty}^{\infty} c_n e^{j2\pi ft} \tag{1}$$

where $c_n = 1/T \int_0^T i_s(t) e^{-j2\pi ft} dt$, and T $(=1/f)$ is the period. c_0 $\left(=1/T \int_0^T i_s(t)\, dt\right)$ is the dc component.

Sample $i_s(t)$ using the sampling rate f_s with N points. Therefore $i_s(t)$ is expressed in a discrete form, that is, $i_s[n]$. Use DFT, and the sequence of $i_s[n]$ is transformed into an N-periodic sequence of complex numbers

$$I_s[k] = \frac{1}{N} \sum_{n=0}^{N-1} i_s[n] e^{-jk2\pi n/N} \tag{2}$$

The inverse DFT is given by

$$i_s[n] = \sum_{k=0}^{N-1} I_s[k] e^{jk2\pi n/N} \tag{3}$$

Assume $i_s(t)$ is a periodic signal and its period is T. The fundamental Fourier angular frequency (ω) is defined as

$$\omega = \frac{2\pi}{T} \tag{4}$$

If the waveform is sampled using p periods where $p > 1$, $\Delta\omega$ can be

represented as

$$\Delta\omega = \frac{2\pi}{pT} = \frac{\omega}{p} \tag{5}$$

Accordingly, the Fourier fundamental frequency (Δf) can be written as

$$\Delta f = \frac{1}{pT} = \frac{1}{pN_sT_s} = \frac{1}{NT_s} = \frac{f_s}{N} \tag{6}$$

where $N_s \triangleq N/p$, $T_s \triangleq 1/f_s$ and f_s is the sampling rate. Note that the Fourier fundamental period is defined as $T_f = 1/\Delta f$.

If the sample window length, that is, the duration of the sampled data vector, is the multiple of fundamental period, the DFT method can be well performed. However, the spectrum leakage problem is unavoidable once the waveforem has a fundamental frequency drift or contains interharmonics. When two steady-state signals, which have constant amplitudes but different frequencies, are linearly superimposed, its time-domain waveform is not necessarily periodic. For example, two frequencies have the relation of non-rational number ($\sqrt{3}$ or$\sqrt{5}$). In addition, Table 1 shows components to form a waveform whch has both harmonics and interharmonics. It can be seen that the waveforms not symmetrical and periodic although every componet is periodic.

2.2 Concept of grouping method

IEC Standard suggests the concept of grouping for measuring the interharmonics [13]. In a 50 Hz power system, the sampling time window is 10 periods, and 60 Hz system is sampled 12 periods. It means that the sampling time takes 200 ms, where the spectrum resolution interval (Δf) is 5 Hz. The profile of IEC subgrouping of 'bins' of harmonics/interharmonics can be seen more details in [13].

By the Parseval relation [39, 40], the power, P, of the waveform can be written as

$$P = \frac{1}{N}\sum_{n=0}^{N-1} i_s[n]^2 = \sum_{k=0}^{N-1} I_s[k]^2 \tag{7}$$

The individual power $P[f_k]$ at the frequency f_k can be written as [39]

$$P[f_k] = I_s[k]^2 + I_s[N-k]^2 = 2I_s[k]^2 \tag{8}$$

where $k = 0,1, 2, \ldots, N/2 - 1$.

The amplitude of mth harmonic at the frequency f_k can be expressed as

$$A_m[f_k] = \sqrt{P[f_k]} = \sqrt{2}I_s[k] \tag{9}$$

where $m = 1,2, \ldots, M$.

The harmonic power at f_k may spill surrounding to neighbours. By the concept of grouping, all dispersed power within adjacent frequencies can be regarded as a 'group power' [13]. In theory, the 'group power', can be restored as

$$P_m^*[f_k] = \sum_{\Delta k=-\tau}^{+\tau} (A_m[f_{k+\Delta k}])^2 \tag{10}$$

where $\tau = 0, 1, 2, 3, \ldots$ is the group bandwidth.

From (10), the harmonic amplitude can be obtained as

$$A_m^*[f_k] = \sqrt{P_m^*[f_k]} \tag{11}$$

Table 1 Components of system waveform

Frequency	Amplitude	Phase, deg
50	1	0
102	0.2	0
121	0.35	0
139	0.1	0
153	0.1	0
250	0.4	0

3 The proposed algorithm

3.1 The relation between harmonic frequency and dispersed energy

Based on the empirical observation, the relation between harmonic frequency and dispersed energy can be induced and defined. Consider the following cases based on DFT analysis. Case 1: Fig. 1*a* reveals that the second larger magnitude ($A_m[f_{k+1}]$) at f_{k+1} is located at the right side of the dominant frequency at f_k, where $A_m[f_k] > A_m[f_{k+1}]$. Generally, f_k may be wrongly interpreted as the dominant harmonic frequency. Actually, it is found that the true frequency known as an interharmonic should be equal to f_k plus the 'frequency deviation' (Δf_k) defined in (12). It is confirmed that higher $A_m[f_{k+1}]$ will introduce more amount of deviation (Δf_k) distant from f_k. Similarly, in Fig. 1*b* Case 2 shows another situation that the second larger amplitude ($A_m[f_k]$) at f_k is located at the left side of the dominant frequency at f_{k+1}, where

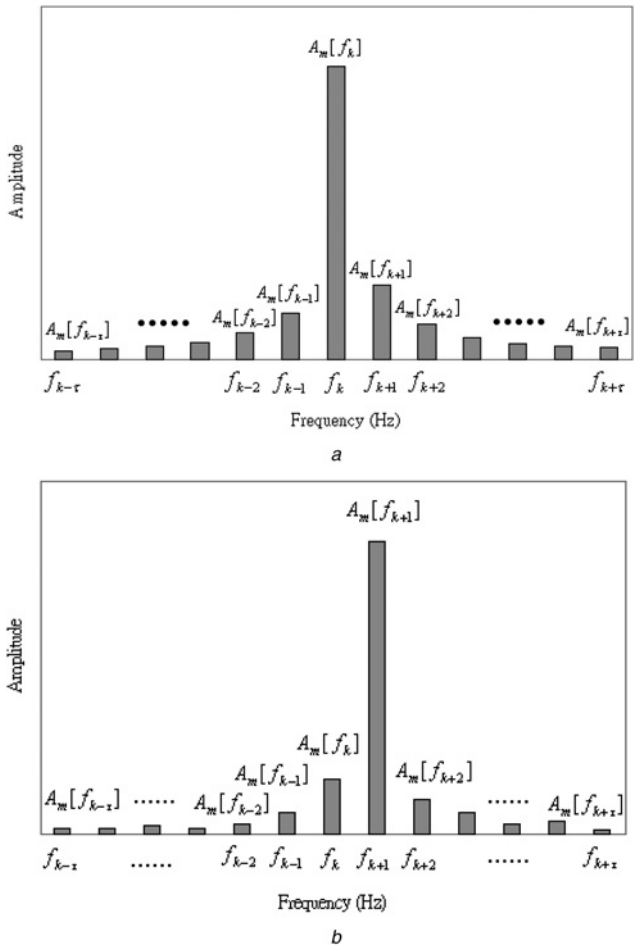

Fig. 1 *Relation between harmonic frequency and dispersed energy*

a Small frequency deviation
b Big frequency deviation

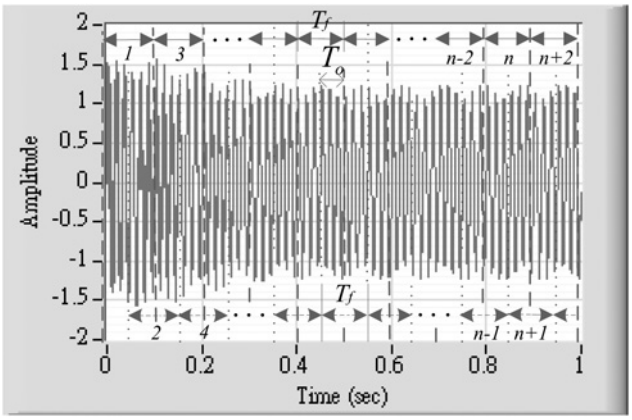

Fig. 2 *Depict of piece-overlapped sampling*

$A_m[f_k] < A_m[f_{k+1}]$. In this case, f_{k+1} may be wrongly interpreted as the dominant harmonic frequency. Like Case 1, the true interharmonic frequency in this case should be equal to f_k plus the 'frequency deviation' (Δf_k). Higher $A_m[f_{k+1}]$ will also introduce more amount of deviation (Δf_k) distant from f_k.

3.2 Proposed leakage energy allocation (LEA) algorithm

Actually, it is very difficult to model the interharmonics using mathematic equations theoretically. Nevertheless, it is found that the frequency deviation amount has a relation with the dispersed energy distribution [25]. Based on the inductive method from empirical results, the frequency of interharmonic can be represented by the dominant frequency (f_k) plus 'frequency deviation' (Δf_k), that is, $f_k + \Delta f_k$. Note that the dominant frequency (f_k) can be directly obtained from DFT. Besides, the principle can be also applied to the system frequency deviation situation.

The frequency deviation range (FDR) is defined as

$$\Delta f_k = \frac{\sqrt{\sum_{\Delta k=1}^{+\tau} A_m[f_{k+\Delta k}]^2}}{\sqrt{\sum_{\Delta k=-\tau}^{0} A_m[f_{k+\Delta k}]^2} + \sqrt{\sum_{\Delta k=1}^{+\tau} A_m[f_{k+\Delta k}]^2}} \Delta f \tag{12}$$

where Δf is a factor of fundamental frequency, that is, 50 Hz. In other words, Δf must be 1, 2, 5, 10, 25, 50.

According to the analysis of group-harmonic frequency deviation, the restored amplitude (RA) can be used for retrieving dispersed amplitude, being defined as

$$\mathrm{RA} = \sqrt{\sum_{\Delta k=-\tau}^{+\tau} A_m[f_{k+\Delta k}]^2} \tag{13}$$

where $\tau = 0, 1, 2, 3, \ldots$.

In order to track time-varying harmonics/interharmonics more rapidly, the piecewise-overlapped method is proposed. The principle is based on the idea of overlapped sampling period. It means that the signal analysed using DFT can be overlapped for a certain period. Therefore it becomes easier to track the variation of dynamic signal. The illustration of this method is shown in Fig. 2. The sampling period is set as T_f, where the number n (=1, 2, 3, 4, …) denotes the sampling sequence with a T_f time period, and next number, that is, $n + 1$, has a overlapped period (T_o) with the current number n.

The overlapped percentage η is defined as the ratio of overlapped period to the sampling sequence as follows

$$\eta = \frac{\text{overlapped period } (T_o)}{\text{sampling period } (T_f)} \tag{14}$$

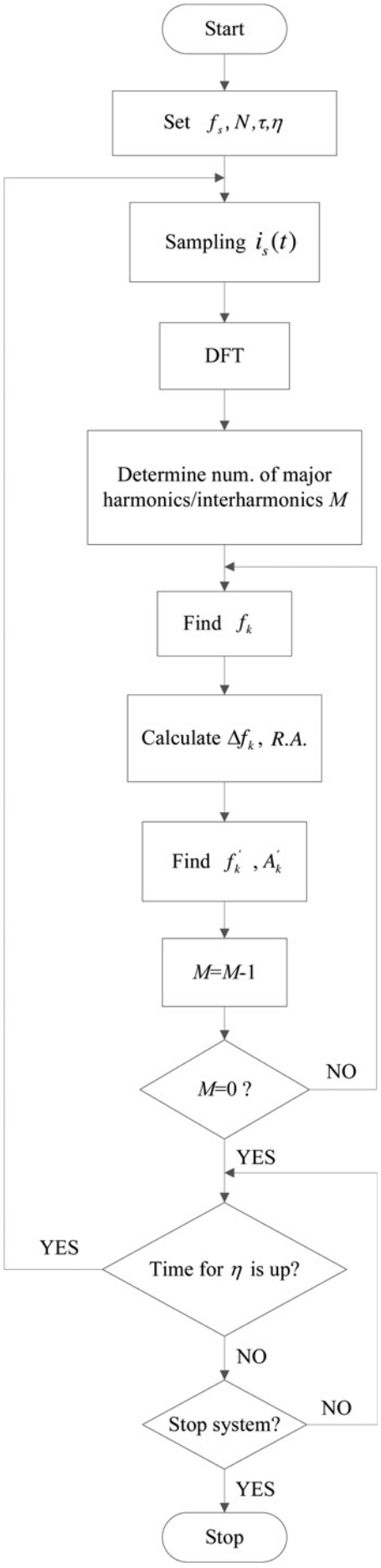

Fig. 3 *Flowchart of the proposed LEA scheme*

IET Gener. Transm. Distrib., 2015, Vol. 9, Iss. 9, pp. 798–804

The flowchart of the proposed LEA algorithm shown in Fig. 3 is described briefly, as follows:

(1) Set f_s, N, τ, η.
(2) Sample the power line waveform $i_s(t)$ using T_f sampling time.
(3) Implement DFT.
(4) Determine the number (M) of dominant harmonics/interharmonics.
(5) Find the location of dominant frequency f_k.
(6) Calculate Δf_k, RA.
(7) Find the respective frequency and amplitude of the harmonic/interharmonic, that is, $f_k' = f_k + \Delta f_k$, $A_k' = \text{RA}$.
(8) $M = M - 1$.
(9) Check if $M = 0$. If yes, continue next step. Otherwise, return to step (5). Note that the procedure is repeated until all harmonics/interharmonics are obtained.
(10) Check if the time for η is up. If yes, go back to step (2). Otherwise, continue next step.
(11) Go back to step (10) until the system is requested to stop.

4 Model validity

The proposed LEA model is based on DFT, and its implementation requires only one more algebra computation step. Therefore the model validity is analogous to the real measurement system using DFT. For this reason, the numerical examples can be used for test with no concession between its potential applications and model validity.

4.1 Stationary waveform analysis with fundamental frequency drift

Firstly, a stationary waveform with fundamental frequency drift is considered. The numerical example that may represent a possible signal distortion situation is employed in this study [41–44]. It indicates that i_a has 0.4 Hz drift at the fundamental frequency (f_1). It also contains two interharmonics (f_2 and f_3)

$$i_a = a_1 \sin(2\pi f_1 t + \varphi_1) + a_2 \sin(2\pi f_2 t + \varphi_2) + a_3 \sin(2\pi f_3 t + \varphi_3) \tag{15}$$

where $f_1 = 49.6$ Hz is the fundamental system frequency that has 0.4 Hz drift from 50 Hz. The f_2 and f_3 are 123, and 327 Hz, respectively. The $a_1 = 1.0$, $a_2 = 0.3$ and $a_3 = 0.15$ are amplitudes. The $\varphi_1 = 0°$, $\varphi_2 = 12°$ and $\varphi_3 = 35°$ are phase degrees.

Consider the case: $\Delta f = 5$ Hz ($f_s = 1$ kHz, $N = 200$, $T_f = 0.2$ s), $\eta = 0$, $\tau = 4$. Spectrum of i_a based on DFT is shown in Fig. 4*a*. It notes that the system frequency and all interharmonics have serious spilled energy around their frequency because of the leakage problem. Using LEA method, the result is accurate, shown in Fig. 4*b*. For details, it is discussed as follows:

a. *System frequency* f_1: Initially, $M = 3$. The FDR beyond 45 Hz can be calculated as (see (16))

$$\Delta f_k = \frac{\sqrt{0.99^2 + 0.07^2 + 0.038^2 + 0.026^2}}{\sqrt{0.024^2 + 0.03^2 + 0.044^2 + 0.088^2} + \sqrt{0.99^2 + 0.07^2 + 0.038^2 + 0.026^2}} \times 5 \simeq \frac{0.994}{0.106 + 0.994} \times 5 \simeq 4.52 \cong 4.5 \tag{16}$$

The 45 Hz (f_k) plus 4.5 Hz (Δf_k) is equal to 49.5 Hz, almost matching the real value ($f_1 = 49.6$ Hz) (see (17))

$$\text{RA} = \sqrt{0.024^2 + 0.03^2 + 0.044^2 + 0.088^2 + 0.99^2 + 0.07^2 + 0.038^2 + 0.026^2} \simeq 1.00 \tag{17}$$

The RA is equal to 1.0, completely matching the real value ($a_1 = 1.0$).

b. *Interharmonic* (f_2): In this stage, $M = 2$. The FDR beyond 120 Hz can be calculated as (see (18))

$$\Delta f_k = \frac{\sqrt{0.22^2 + 0.062^2 + 0.035^2 + 0.024^2}}{\sqrt{0.028^2 + 0.038^2 + 0.059^2 + 0.15^2} + \sqrt{0.22^2 + 0.062^2 + 0.035^2 + 0.024^2}} \times 5 \simeq \frac{0.236}{0.172 + 0.236} \times 5 \simeq 2.89 \cong 3 \tag{18}$$

The 120 Hz (f_k) plus 3 Hz (Δf_k) is equal to 123 Hz, matching the real value ($f_2 = 123$ Hz) (see (19))

$$\text{RA} = \sqrt{0.028^2 + 0.038^2 + 0.059^2 + 0.15^2 + 0.22^2 + 0.062^2 + 0.035^2 + 0.024^2} \simeq 0.29 \cong 0.3 \tag{19}$$

The RA is almost equal to 0.3, matching the real value ($a_2 = 0.3$).

c. *Interharmonic* (f_3): In this stage, $M = 1$. The FDR beyond 325 Hz can be calculated as (see (20))

$$\Delta f_k = \frac{\sqrt{0.076^2 + 0.028^2 + 0.018^2 + 0.013^2}}{\sqrt{0.013^2 + 0.019^2 + 0.032^2 + 0.11^2} + \sqrt{0.076^2 + 0.028^2 + 0.018^2 + 0.013^2}} \times 5 \simeq \frac{0.0835}{0.12 + 0.0835} \times 5 \simeq 2.05 \cong 2 \tag{20}$$

The 325 Hz (f_k) plus 2 Hz (Δf_k) is almost equal to 327 Hz, matching the real value ($f_3 = 327$ Hz) (see (21))

$$\text{RA} = \sqrt{0.013^2 + 0.019^2 + 0.032^2 + 0.11^2 + 0.076^2 + 0.028^2 + 0.018^2 + 0.013^2} \simeq 0.146 \cong 0.15 \tag{21}$$

The RA is very close to 0.15, matching the real value ($a_3 = 0.15$). After this process, $M = 0$ so that the calculation of individual frequency and amplitude stops.

Some more cases using $\Delta f = 1$, 2, 10 and 25 Hz, respectively, have been also tested and achieved similar performance outcomes. It is concluded in Table 2. Obviously, DFT cannot give an accurate solution except f_2 and f_3 components using $\Delta f = 1$ Hz. For the proposed LEA scheme, all components identification using $\Delta f = 1$, 2, 5, 10 Hz can achieve a very correct value for either frequency or amplitude. On the other hand, Δf using 25 Hz is unable to obtain a satisfactory result because of no remarkable adjacent dispersed energy. Actually, it is clear that the sampling time (T_f) will be reduced if a large Δf up to 10 Hz is chosen, not paying the cost of accuracy. However, in a view of general practice, the risk of reciprocal interference between surrounding harmonics/

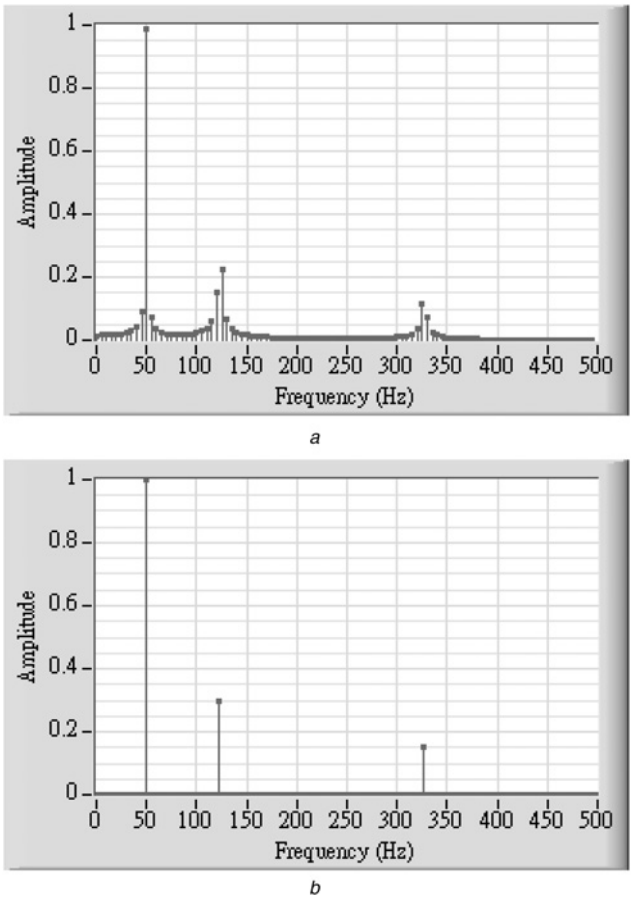

Fig. 4 *Spectrum of i_a using $\Delta f = 5$ Hz*
a Spectrum of i_a with DFT
b Spectrum of i_a with LEA

interharmonics spilled energy may arise once a larger Δf is used. To reach a compromise, $\Delta f = 5$ Hz is taken an account in this study.

4.2 Non-stationary waveform tracking analysis

For non-stationary waveform analysis, we set $\Delta f = 5$ Hz, $\eta = 0.5$ and $\tau = 4$ for time-variant frequency and amplitude tracking.

4.2.1 Time-variant frequency tracking: In order to verify the capability of time-variant frequency tracking with the proposed algorithm, the waveform of i_a (t) using (22) has been tested

$$i_a(t) = a_1 \sin(2\pi f_1 t + \phi_1) + a_2 \sin(2\pi f_2 t + \phi_2) + a_3 \sin(2\pi f_3 t + \phi_3) \quad (22)$$

where $a_1 = 1.0$, $a_2 = 0.23$, $a_3 = 0.14$, $f_1 = 50$ Hz, $f_2 = 29$ Hz, $f_3 = 122$ Hz, $\phi_1 = 8°$, $\phi_2 = 52°$, $\phi_3 = 23°$.

Assume that the waveform frequency components of i_a (t) change every 0.1 s, as follows. The frequency tracking curve using LEA is shown in Fig. 5. We see that each frequency variety can be tracked successfully

1. $t = 0.0$ s : $f_2 = 29$ Hz, $f_3 = 122$ Hz;
2. $t = 0.1$ s : $f_2 = 28$ Hz, $f_3 = 124$ Hz;
3. $t = 0.2$ s : $f_2 = 25$ Hz, $f_3 = 121$ Hz;
4. $t = 0.3$ s : $f_2 = 34$ Hz, $f_3 = 120$ Hz;
5. $t = 0.4$ s : $f_2 = 35$ Hz, $f_3 = 113$ Hz;
6. $t = 0.5$ s : $f_2 = 38$ Hz, $f_3 = 117$ Hz;
7. $t = 0.6$ s : $f_2 = 37$ Hz, $f_3 = 114$ Hz;
8. $t = 0.7$ s : $f_2 = 33$ Hz, $f_3 = 117$ Hz;
9. $t = 0.8$ s : $f_2 = 32$ Hz, $f_3 = 120$ Hz;
10. $t = 0.9$ s : $f_2 = 31$ Hz, $f_3 = 115$ Hz;
11. $t = 1.0$ s : $f_2 = 30$ Hz, $f_3 = 122$ Hz.

4.2.2 Time-variant amplitude tracking: Consider the situation with time-variant amplitude using (23), and the waveform of $i_b(t)$ is

Table 2 Result comparison between DFT and LEA

Δf										
Real values	$\Delta f = 1$ Hz		$\Delta f = 2$ Hz		$\Delta f = 5$ Hz		$\Delta f = 10$ Hz		$\Delta f = 25$ Hz	
	DFT	LEA	DFT	LEA	DFT	LEA	DFT	LEA	DFT	LEA
$f_1 = 49.6$, Hz	49	49.6	48	49.6	45	49.5	40	49.5	50	50
$f_2 = 123$, Hz	123	123	122	123	120	123	120	123	125	127
$f_3 = 327$, Hz	327	327	326	327	325	327	320	327	300	322
$a_1 = 1.0$	1.0	1.01	0.93	1.03	0.99	1.00	1.0	1.02	1.0	1.0
$a_2 = 0.3$	0.3	0.3	0.19	0.29	0.22	0.29	0.26	0.29	0.31	0.31
$a_3 = 0.15$	0.15	0.15	0.095	0.146	0.076	0.146	0.13	0.148	0.15	0.16

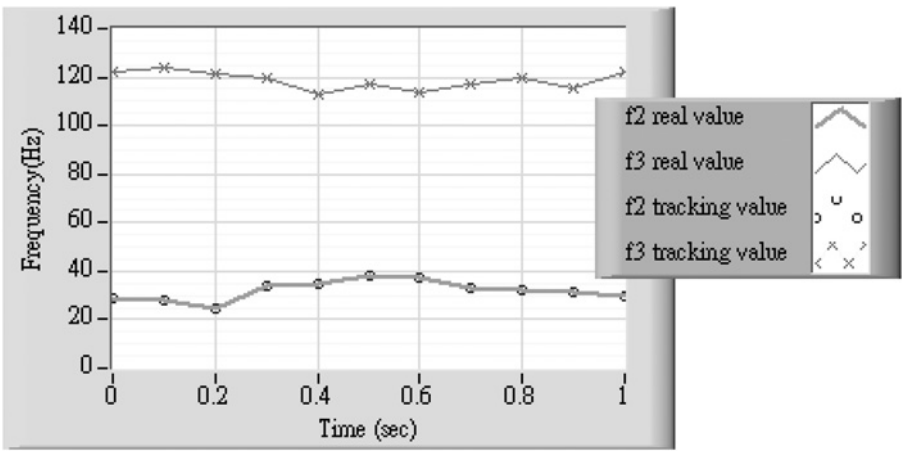

Fig. 5 *Frequency tracking curve of $i_a(t)$*

IET Gener. Transm. Distrib., 2015, Vol. 9, Iss. 9, pp. 798–804

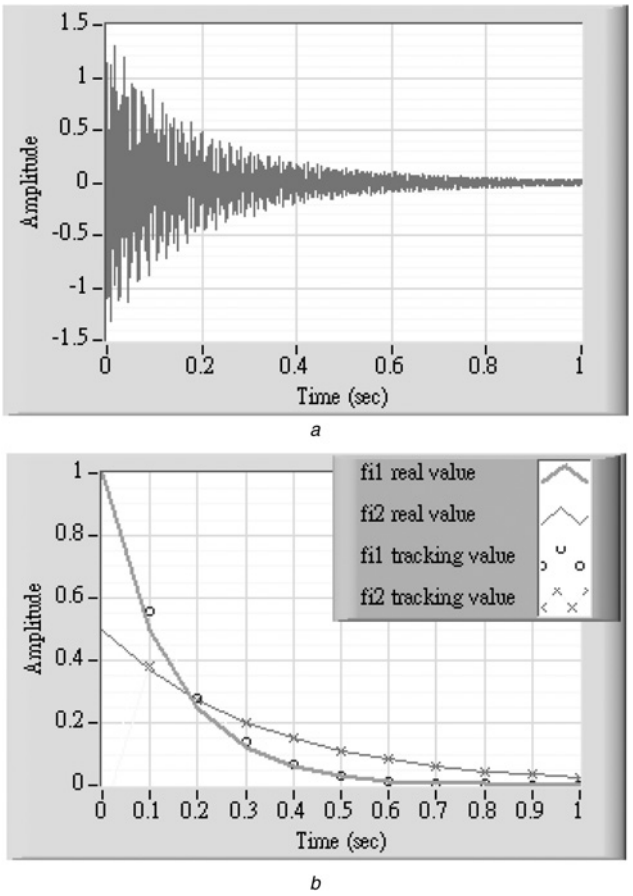

Fig. 6 *Waveform changing of $i_b(t)$*

a Waveform of $i_b(t)$
b Amplitude tracking curve

shown in Fig. 6*a*. Its amplitude that contains both interharmonics (312 and 425 Hz with different time constants) is decaying down to zero within 1 s. From the results shown in Fig. 6*b*, it is obvious that the amplitude can be also tracked successfully

$$i_b(t) = a\sin(2\pi f_{i1}t)\mathrm{e}^{-t/T_{c1}} + b\sin(2\pi f_{i2}t)\mathrm{e}^{-t/T_{c2}} \quad (23)$$

where $a = 1$, $f_{i1} = 312$ Hz, $1/T_{c1} = 7$, $b = 0.5$, $f_{i2} = 425$ Hz, $1/T_{c2} = 6$.

As above, the changes in both time-variant amplitude and frequency are tested using the same interval, that is, 0.1 s. It is realised that the proposed model computes both interharmonic amplitude and frequency at the same time. Consequently, it is obvious that simultaneous frequency and amplitude changes can be tracked simultaneously.

4.3 Discussion for selection of group bandwidth (τ)

Interharmonics is asynchronous with fundamental and harmonics so that using DFT for spectrum analysis will cause spectral leakage if the waveform contains interharmonics. In such a situation, the power of the harmonic at f_k may disperse over a frequency band. It is noted that the larger group bandwidth (τ) may restore all leakages and thus regain the actual amplitude/frequency. However, with a large bandwidth the 'group power' may cover some harmonic contents at distant frequencies. For this reason, the group bandwidth (τ) should be chosen as large as possible but small enough to avoid the overlap between two neighbouring harmonic groups. Based on this principle, τ is chosen as 4 for selecting $\Delta f = 1$, 2 and 5 Hz, and τ is chosen as 3 for selecting $\Delta f = 10$ Hz. However, τ should be set as 1 for $\Delta f = 25$ Hz to exclude possible dispersed power interaction.

5 Conclusions

The DFT is still widely used in signal measurement in industry. However, it may not be applicable in some circumstances such as non-stationary or interharmonics analysis. This paper has developed an LEA approach for both stationary and non-stationary interharmonics evaluation in power systems. It can recover all spilled leakage energy to obtain its original interharmonics amplitude. Also, every individual frequency component can be calculated using the principle of the distribution state of spilled leakage energy. In this study, $\Delta f = 5$ Hz is selected for the trade-off between the sampling time and measurement accuracy. The piecewise-overlapped method that is integrated with the LEA scheme can be used to track the signal variation more quickly. For industrial applications, the implementation cost of the proposed LEA is lower than traditional grouping methods, where it only requires one more number of operation than DFT. Also, no extended memory is needed in general computers or microprocessors. Accordingly, it can be easily applied to DFT-based instruments owing to its simple mathematics basis of DFT. For future work, it recommends that this research can be extended and focused on the separation or interfere from spectral leakage between very close harmonics and interharmonics.

6 References

1 Lin, H.C.: 'Sources, effects and modelling of interharmonics', *Math. Probl. Eng.*, 2014, **2014**, pp. 1–10
2 Qian, H., Ahao, R., Chen, T.: 'Interharmonics analysis based on interpolating windowed FFT algorithm', *IEEE Trans. Power Deliv.*, 2007, **22**, (2), pp. 1064–1069
3 Rifai, M.B., Ortmeyer, T.H., McQuillan, W.J.: 'Evaluation of current interharmonics from AC drives', *IEEE Trans. Power Deliv.*, 2000, **15**, (3), pp. 1094–1098
4 Zhang, Q., Liu, H., Chen, H., Li, Q., Zhang, Z.: 'A precise and adaptive algorithm for interharmonics measurement based on iterative DFT', *IEEE Trans. Power Deliv.*, 2008, **23**, (4), pp. 1728–1735
5 Testa, A., Akram, M.F., Burch, R., *et al.*: 'Interharmonics: Theory and modeling', *IEEE Trans. Power Deliv.*, 2007, **22**, (4), pp. 2335–2348
6 Lin, H.C.: 'Fast tracking of time-varying power system frequency and harmonics using iterative-loop approaching algorithm', *IEEE Trans. Ind. Electron.*, 2007, **54**, (2), pp. 974–983
7 Sueker, K.H., Hummel, S.D., Argent, R.D.: 'Power factor correction and harmonic mitigation in a thyristor controlled glass melter', *IEEE Trans. Ind. Appl.*, 1989, **25**, (6), pp. 972–975
8 Steeper, D.E., Stratford, R.P.: 'Reactive compensation and harmonic suppression for industrial power systems using thyristor converters', *IEEE Trans. Ind. Appl.*, 1976, **IA-12**, (3), pp. 232–254
9 Barros, J., Prez, E., Pigazo, A., Diego, R.I.: 'Simultaneous measurement of harmonics, interharmonics and flicker in a power system for power quality analysis'. Fifth Int. Conf. Power System Management and Control, April 2002, pp. 100–105
10 Gallo, D., Langella, R., Testa, A.: 'Interharmonics, Part 1: Aspects related to modeling and simulation'. Sixth Int. Workshop on Power Definitions and Measurements under Non-Sinusoidal Conditions, Milano, October 2003, pp. 168–173
11 Karimi-Ghartemani, M., Iravani, M.R.: 'Measurement of harmonics/inter-harmonics of time-varying frequency', *IEEE Trans. Power Deliv.*, 2005, **20**, (1), pp. 23–31
12 Gallo, D., Langella, R., Testa, A.: 'Interharmonics, Part 2: aspects related to measurement and limits'. Sixth Int. Workshop on Power Definitions and Measurements under Non-Sinusoidal Conditions, Milano, October 2003, pp. 174–181
13 IEC 61000-4-7: Electromagnetic compatibility (EMC) Part 4: testing and measurement techniques Section 7: general guide on harmonics and interharmonics measurements and instrumentation for power supply systems and equipment connected thereto, 2002
14 Li, C., Xu, W., Tayjasanant, T.: 'Interharmonics: basic concepts and techniques for their detection and measurement', *Electr. Power Syst. Res.*, 2003, **66**, (1), pp. 39–48
15 Lin, H.C.: 'Intelligent neural network based adaptive power line conditioner for real-time harmonics filtering', *IEE Proc.-Gener. Transm. Distrib.*, 2004, **151**, (5), pp. 561–567
16 Moo, C.S., Chang, Y.N.: 'Group-harmonic identification in power systems with nonstationary waveforms', *IEE Proc.-Gener. Transm. Distrib.*, 1995, **142**, (5), pp. 517–522
17 Chen, S., Lai, Y.M., Tan, S.-C., Tse, C.K.: 'Fast response low harmonic distortion control scheme for voltage source inverters', *IET Power Electron.*, 2009, **2**, (5), pp. 574–584
18 Madhan, M.D., Singh, B., Panigrahi, B.K.: 'Harmonic optimised 24-pulse voltage source converter for high voltage DC systems', *IET Power Electron.*, 2009, **2**, (5), pp. 563–573

19 Kwok, H.K., Jones, D.L.: 'Improved instantaneous frequency estimation using an adaptive short-time Fourier transform', *IEEE Trans. Signal Process.*, 2000, **48**, (10), pp. 2964–2972
20 Macias, J.A., Gomez, A.: 'Self-tuning of Kalman filters for harmonic computation', *IEEE Trans. Power Deliv.*, 2006, **21**, (1), pp. 501–503
21 Lin, H.C.: 'Intelligent neural network based fast power system harmonic detection', *IEEE Trans. Ind. Electron.*, 2007, **54**, (1), pp. 43–52
22 Bettayeb, M., Qidwai, U.: 'Recursive estimation of power system harmonics', *Elect. Power Syst. Res.*, 1998, **47**, pp. 143–152
23 Soliman, S.A., Alammari, R.A., El-Hawary, M.E., Mostafa, M.A.: 'Effects of harmonic distortion on the active and reactive power measurements in the time dominant: a single phase system'. 2001 IEEE Porto Power Tech Conf., Porto, September 2001, pp. 1–6
24 Chang, G.W., Chen, C.I., Liu, Y.J., Wu, M.C.: 'Measuring power system harmonics and interharmonics by an improved fast Fourier transform-based algorithm', *IET Gener. Transm. Distrib.*, 2008, **2**, (2), pp. 193–201
25 Lin, H.C.: 'Inter-harmonic identification using group-harmonic weighting approach based on the FFT', *IEEE Trans. Power Electron.*, 2008, **23**, (3), pp. 1309–1319
26 Javier, V., Jorge, P.: 'Real-time interharmonics detection and measurement based on FFT algorithm'. Applied Electronics, Pilsen, 2009, pp. 259–264
27 Chang, G.W., Chen, C.-I., Liang, Q.-W.: 'A two-stage ADALINE for harmonics and interharmonics measurement', *IEEE Trans. Ind. Electron.*, 2009, **56**, (6), pp. 2220–2228
28 Gu, I.Y.-H., Kim, T., Powers, E.J., Grady, W.M., Arapostathis, A.: 'Detection of flicker caused by interharmonics', *IEEE Trans. Instrum. Meas.*, 2009, **58**, (1), pp. 152–160
29 Singh, G.K.: 'Power system harmonics research: a survey', *Eur. Trans. Electr. Power*, 2009, **19**, (2), pp. 151–172
30 Chen, C.-I., Chang, G.W.: 'Virtual instrumentation and educational platform for time-varying harmonic and interharmonic detection', *IEEE Trans. Ind. Electron.*, 2010, **57**, (10), pp. 3334–3342
31 Chang, G.W., Chen, S.-K., Su, H.-J., Wang, P.-K.: 'Accurate assessment of harmonic and interharmonic currents generated by VSI-Fed drives under unbalanced supply voltages', *IEEE Trans. Power Deliv.*, 2011, **26**, (2), pp. 1083–1091
32 Nassif, A.B., Yong, J., Mazin, H., Wang, X., Xu, W.: 'An impedance-based approach for identifying interharmonic sources', *IEEE Trans. Power Deliv.*, 2011, **26**, (1), pp. 333–340
33 Ramirez, A.: 'The modified harmonic domain: interharmonics', *IEEE Trans. Power Deliv.*, 2011, **26**, (1), pp. 235–241
34 Lin, H.C.: 'Power harmonics and interharmonics measurement using recursive group-harmonic power minimizing algorithm', *IEEE Trans. Ind. Electron.*, 2012, **59**, (2), pp. 1184–1193
35 Hajibeigy, M., Farsadi, M., Nazarpour, D., Golahmadi, H., Hajibeigy, M.: 'Harmonic suppression in HVDC system using a modified control method for hybrid active DC filter', *Eur. Trans. Electr. Power*, 2012, **22**, (3), pp. 294–307
36 Sadinezhad, I., Agelidis, V.G.: 'Real-time power system phasors and harmonics estimation using a new decoupled recursive-least-squares technique for DSP implementation', *IEEE Trans. Ind. Electron.*, 2013, **60**, (6), pp. 2295–2308
37 Jain, S.K., Singh, S.N.: 'Fast harmonic estimation of stationary and time-varying signals using EA-AWNN', *IEEE Trans. Instrum. Meas.*, 2013, **62**, (2), pp. 335–343
38 Lin, H.C.: 'Accurate harmonic/inter-harmonic estimation using DFT-based group-harmonics energy diffusion algorithm', *Can. J. Electr. Comput. Eng.*, 2014, **36**, (4), pp. 158–171
39 Oppenheim, A.V., Schafer, R.W.: 'Discrete-time signal processing' (Prentice-Hall, 1989)
40 Press, W.H., Flannery, B.P., Teukolsky, S.A., Vetterling, W.T.: 'Numerical recipes – the art of scientific computing' (Cambridge University, Cambridge, 1986), pp. 420–429
41 Nguyen, T.T.: 'Parametric harmonic analysis', *IEE Proc.-Gener. Transm. Distrib.*, 1997, **144**, (1), pp. 21–25
42 Pham, V.L., Wong, K.P.: 'Wavelet-transform-based algorithm for harmonic analysis of power system waveforms', *IEE Proc.-Gener. Transm. Distrib.*, 1999, **146**, (3), pp. 249–254
43 Lin, H.C., Lee, C.S.: 'Enhanced FFT based parametric algorithm for simultaneous multiple harmonics analysis', *IEE Proc.-Gener. Transm. Distrib.*, 2001, **148**, pp. 209–214
44 Lin, H.C.: 'Power harmonics and interharmonics measurement using recursive group-harmonic power minimizing algorithm', *IEEE Trans. Ind. Electron.*, 2012, **59**, (2), pp. 1184–1193